Biochemical and Biophysical Research Communications 403 (2010) 1–6

Contents lists available at ScienceDirect

Biochemical and Biophysical Research Communications

journal homepage: www.elsevier.com/locate/ybbrc

Regulatory light chains modulate *in vitro* actin motility driven by skeletal heavy meromyosin

N.N. Vikhoreva, A. Månsson *

School of Natural Sciences, Linnaeus University, SE-391 82 Kalmar, Sweden

ARTICLE INFO

Article history:
Received 1 October 2010
Available online 12 October 2010

Keywords:
In vitro motility assay
Skeletal muscle myosin
Regulatory light chains
Surface charge
Nanotechnological applications
Contact angle

ABSTRACT

Phosphorylation and Ca^{2+}–Mg^{2+} exchange on the regulatory light chains (RLCs) of skeletal myosin modulate muscle contraction. However, the relation between the mechanisms for the effects of phosphorylation and metal ion exchange are not clear. We propose that modulation of skeletal muscle contraction by phosphorylation of the myosin regulatory light chains (RLCs) is mediated by altered electrostatic interactions between myosin heads/necks and the negatively charged thick filament backbone. Our study, using the *in vitro* motility assay, showed actin motility on hydrophilic negatively charged surfaces only over the HMM with phosphorylated RLCs both in the presence and absence of Ca^{2+}. In contrast, good actin motility was observed on silanized surfaces (low charge density), independent of RLC phosphorylation status but with markedly lower velocity in the presence of Ca^{2+}. The data suggest that Ca^{2+}-binding to, and phosphorylation of, the RLCs affect the actomyosin interaction by independent molecular mechanisms. The phosphorylation effects depend on hydrophobicity and charge density of the underlying surface. Such findings might be exploited for control of actomyosin based transportation of cargoes in lab-on-a chip applications, e.g. local and temporary stopping of actin sliding on hydrophilic areas along a nanosized track.

1. Introduction

Skeletal muscle myosin II has two heavy chains that each consists of a C-terminal coiled-coil rod and a globular head at the N-terminus (Supplementary Fig. 1). One essential light chain (ELC) and one regulatory light chain (RLC) stabilize [1,2] the α-helical neck domain that connects the head to the rod. In muscle contraction, globular motor domains (heads) of myosin II molecules interact cyclically with actin filaments to form actomyosin cross-bridges which transduce the energy of ATP hydrolysis into force and movement [3]. In mammalian smooth muscle and non-muscular cells, as well as in most non-mammalian skeletal muscles, myosin based contraction/motility is switched on by phosphorylation of the RLCs [4] or by Ca^{2+} binding to the ELCs [5]. In mammalian striated muscle (skeletal muscle, heart), on the other hand, contraction is turned on by Ca^{2+}-binding to the troponin–tropomyosin complex on the thin filaments [6]. However, also in these myosins, the RLCs are phosphorylated during contraction, particularly during extended activity [7]. Moreover, the Mg^{2+} ion in a divalent cation binding site on the RLC [8] is exchanged for Ca^{2+} during extended periods with raised intracellular Ca^{2+}-levels [9].

Phosphorylation of, and Ca^{2+}-binding to, the RLCs in striated muscle seem to be of physiological relevance (e.g. [10,11]) and the phenomena have been extensively studied [7,9,12–17]. Phosphorylation dependent force potentiation appears to result from recruitment of actomyosin cross-bridges due to movement of myosin heads away from the thick filament backbone [7,18] (formed mainly by myosin rods). Exchange of Mg^{2+} for Ca^{2+} on the divalent cation binding sites of the RLCs seems to have similar effects [6,12,19]. In the case of the phosphorylation effects, it has been proposed that the extra negative charges introduced by the phosphate group, may cause the myosin heads to swing away from their relaxed, "parked", state, due to altered electrostatic interactions with the negatively charged thick filament backbone [13,17]. This down-stream mechanism cannot readily account for the effect of Ca^{2+}–Mg^{2+} exchange, but the possibility of cooperativity between the effects of phosphorylation and Ca^{2+}–Mg^{2+} exchange has been considered [9,11,12,16,20].

If the phosphorylation effects are due to altered electrostatic interactions, as outlined above, one could imagine similar effects of RLC phosphorylation on the interaction between surface-adsorbed heavy meromyosin (HMM) and negatively charged surfaces. This would open for exploitation of phosphorylation-dephosphorylation induced changes in the RLCs for *in vitro* control

Abbreviations: RLC, regulatory light chain; ELC, essential light chain; HMM, heavy meromyosin; pHMM, HMM with phosphorylated RLCs; upHMM, HMM with unphosphorylated RLCs; TMCS, trimethylchlorosilane; MLCK, myosin light chain kinase.

* Corresponding author. Fax: +46 480 446262.
E-mail address: alf.mansson@lnu.se (A. Månsson).

0006-291X/$ - see front matter © 2010 Elsevier Inc. All rights reserved.
doi:10.1016/j.bbrc.2010.10.039

of HMM induced actin motility on artificial surfaces, e.g. in recently proposed nanotechnological applications [21–25]).

In support of the above hypotheses we found HMM propelled actin filament sliding on highly negatively charged surfaces [26] only when the RLCs were phosphorylated. In contrast, on hydrophobic surfaces of lower surface charge density, high-quality actin sliding was observed with both unphosphorylated and phosphorylated RLCs. On the latter type of surface Ca^{2+}–Mg^{2+} exchange on the RLCs reduced sliding velocity, independent of the phosphorylation effects.

A model to account for the observed effects of RLC-phosphorylation is presented. Further, the potential for nanotechnological applications and the possible interaction between effects of phosphorylation and Ca^{2+}–Mg^{2+} exchange is discussed.

2. Materials and Methods

2.1. Protein preparations

Fast skeletal muscle myosin with phosphorylated and unphosphorylated RLCs was obtained from rabbit back muscle [27]. Heavy meromyosin (HMM) [28] and skeletal muscle actin [29] were prepared as described previously. The HMM (3 different preparations) was drop-frozen in liquid nitrogen and stored at -80 °C between experiments. The extent of RLC-phosphorylation (close to 0 and 100% for unphosphorylated and phosphorylated HMM, respectively) was verified by 8 M urea gel electrophoresis [30] of myosin and HMM (Supplementary Fig. 2) before and after freezing.

2.2. Surface preparations and contact angle measurements

Glass coverslips (Menzel-Gläser, Braunshweig, Germany; *cf.* [31]) for *in vitro* motility assays, were treated to obtain surfaces with different hydrophobicity (related to surface charge density; [26]) as quantified by the contact angle with water droplets [32]. A hydrophilic surface with contact angle of 10 ± 2° was obtained by treatment with Piranha solution (70% H_2SO_4 and 10% H_2O_2) for 6 min at 80 °C (see [33] for handling details), followed by rinsing several times with superQ water. A contact angle of 30 ± 2 ° was obtained by sonication for 30 min in 70% ethanol. Coverslips rinsed in 70% ethanol solution for 1 min had a contact angle of 50 ± 2°. Finally, a surface with contact angle of 70 ± 2 ° was obtained by silanization with trimethylchlorosilane (TMCS; [33,34]). Such surfaces have been shown to have a negative charge density, approximately half of that for Piranha cleaned glass surfaces [26].

2.3. In vitro motility assays

In vitro motility assays were performed essentially as described previously [28]. The HMM was diluted to 120 μg/ml in a buffer (ionic strength 130 mM) of composition (mM): MOPS 10 (pH 7.4), DTT 10, $MgCl_2$ 1, EGTA 0.1, KCl 115 and $CaCl_2$ 0.3 (free Ca^{2+} 0.2) or EGTA 1 (free Ca^{2+} 0). The assay buffer had a similar composition but also contained 1 mM MgATP, 0.5% methylcellulose, 3 mg/ml glucose, 100 μg/ml glucose oxidase and 20 μg/ml catalase. The motility assays were performed at 26 ± 0.5 °C. The number density (ρ) of actin propelling myosin heads was estimated by fitting data for sliding velocity against filament length by the equation [35]:

$$v = v_0(1 - (1 - f)^{\rho Ld}) \quad (1)$$

Here, v_0 is the velocity for filaments being long enough to have at least one actin propelling myosin head attached all the time. Further, the quantity f, is the duty ratio (the fraction of the ATPase cycle time that myosin spends attached in a force-generating state), L is the actin filament length and d is the width of a band around the filament where the myosin heads are within reach for attachment. In the present fittings, f was fixed to 0.05 [35], d to 30 nm [35] and v_0 was the average velocity for long actin filaments. The *in vitro* motility assay data were recorded and analyzed as described in [36]. Actin filament length was estimated from the total filament intensity [31] for a subpopulation of all image sequences. This allowed imaging in the same sequence of filaments analyzed with respect to velocity and of the long (~3–11 μm) filaments, used for calibration of the intensity-length relation.

2.4. Statistical analysis

All data are expressed as mean and standard error of the mean (mean ± SEM). Statistical hypothesis testing was performed using analysis of variance (ANOVA) on the assumption that each filament represents an independent random sample. Statistical analyses, were performed using GraphPad Prism software (version 5.01, GraphPad Software, San Diego, CA, USA).

3. Results and Discussion

There was a clear trend (Fig. 1) for reduced actin sliding velocity with reduced contact angle of the HMM adsorbing surface for all incubation conditions (slopes different from zero; $p < 0.05$). On the surfaces of highest contact angle (70 °; TMCS), actin filaments were propelled with slightly lower velocity by phosphorylated HMM (pHMM) than by unphosphorylated HMM (upHMM; Fig. 1 A, B). The effect of Ca^{2+} on velocity was more substantial (Fig. 1 C, D) with marked reduction in sliding velocity on TMCS surfaces for both pHMM and upHMM. Both the effects of Ca^{2+} and phosphorylation on velocity were statistically significant ($p < 0.001$) and there was no interaction ($p \approx 0.16$) between the effects (two-way ANOVA).

A substantially larger fraction of the actin filaments was propelled by pHMM than by upHMM on surfaces of low (< 50 °) contact angle (Fig. 2) and the sliding velocity was higher with pHMM under these conditions (Fig. 1 A, B). Interestingly, the total fraction of motile filaments with pHMM was as high on the surfaces of lowest contact angle as on the TMCS surface with a contact angle of 70 ° (Fig. 2 A, B). In contrast, this fraction was very low with upHMM in the absence of Ca^{2+} and, whereas there seemed to be more actin binding for upHMM on surfaces of low contact angle in the presence of Ca^{2+}, the filaments were generally sliding too erratically (with stops, pauses and excessive Brownian motion; Supplementary Fig. 3) to be defined as motile in the analysis in Figs. 1 and 2. The results suggest that phosphorylation of the RLCs rescues motility on surfaces of low contact angle (high negative charge density) independent of whether Ca^{2+} is present or not. A similar phosphorylation induced effect was not seen if reduced motility was attributed to reduced HMM surface density on TMCS (Fig. 2C; see further below).

Overall, the above results suggest independent effects of phosphorylation and Ca^{2+}-binding to the RLCs. This is in contrast to ideas that these effects exhibit cooperativity [9,11,12,16,20]. Possibly, whether there is independence or cooperativity may be determined by differences between experimental systems. Thus, in contrast to earlier work using full length myosin, the most C-terminal part (the light meromyosin part) of the myosin tail is not present in HMM that we used here. This also, necessarily, removed any effects attributed to interactions between the myosin heads and a myosin filament backbone.

On surfaces with optimal motility quality (TMCS), phosphorylation of the RLCs had a small reducing effect on the sliding velocity that was intermediate between the 20–30% reduction with full length myosin *in vitro* [14] and the total lack of effects of RLC phosphorylation on velocity in muscle fibers under physiological conditions ([15] and references therein). Thus, again, the results suggest

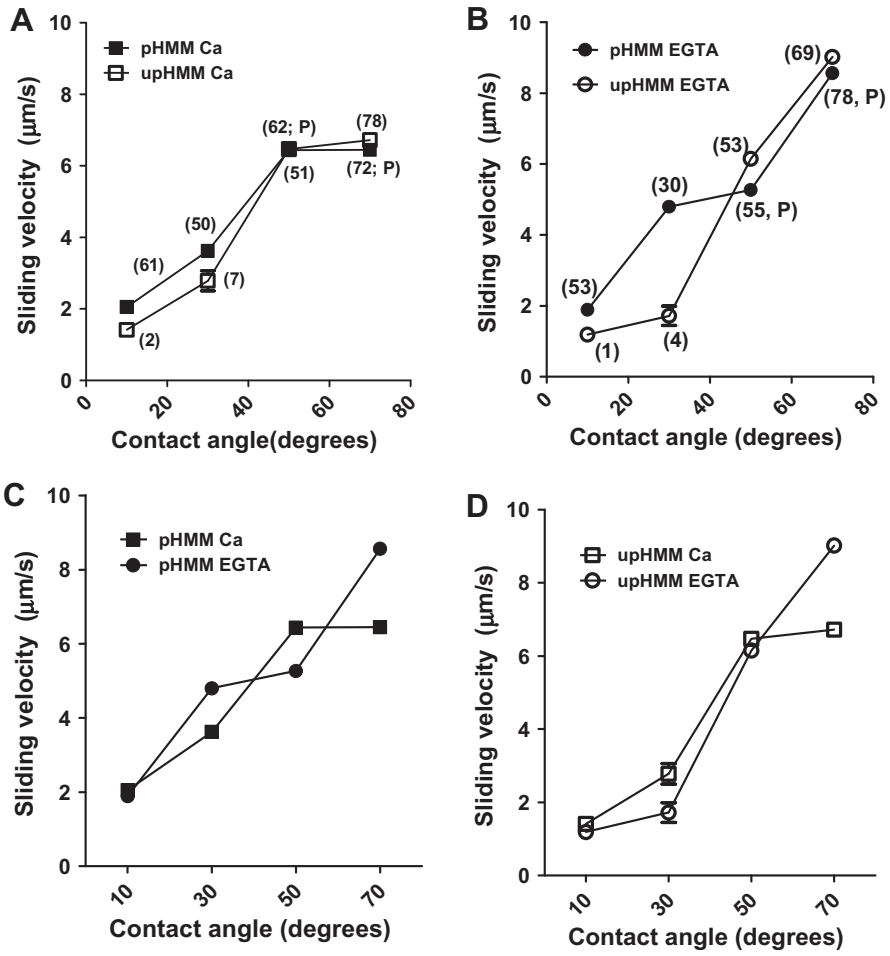

Fig. 1. Sliding velocity of actin filaments (propelled by pHMM or upHMM), plotted against contact angles of the surfaces. (A) In the presence of Ca^{2+}, (B) in the presence of EGTA, ([Ca^{2+}] = 0 mM), (C) pHMM with Ca^{2+} or EGTA, (D) upHMM with Ca^{2+} or EGTA. Number of filaments given within parentheses in A and B. Pooled data from three different HMM preparations and different experimental dates.

that the experimental system influences RLC mediated effects (*cf.* [11] for Discussion of related ideas).

Effects of Ca^{2+} on the velocity of HMM propelled actin filaments (Fig. 1C, D) has not previously been demonstrated in the absence of thin filament regulatory proteins (troponin and tropomyosin) and the effect on velocity is also opposite to that seen upon addition of Ca^{2+} to thin filaments. Clearly, the effect is not due to a reduced density of actin propelling HMM molecules (Supplementary Fig. 4) but the available evidence (Supplementary Discussion) suggests that it is attributed to exchange of Mg^{2+} for Ca^{2+} on the RLCs. The independence of the phosphorylation and Ca^{2+} effects suggests different and independent mechanisms with the phosphorylation effects seemingly related to altered interactions with the underlying surfaces and increased head mobility (see below). Whereas it would be of great relevance [10] to elucidate the mechanism for the Ca^{2+}–Mg^{2+} exchange in greater detail this is beyond the scope of the present investigation.

Previous investigations of HMM induced actin motility on different surface substrates [21,26,31,34,37,38] have been limited to HMM prepared to be predominantly unphosphorylated. These studies showed no, or very limited, motility on glass surfaces of contact angle <30° and a nearly linear increase in sliding velocity with contact angle in the range 30–70° [26]. As expected, these findings are similar to the results using upHMM in Fig. 1D and Fig. 2 A, B. In order to understand the effects of RLC-phosphorylation at different contact angles it is important to consider the present level of understanding for upHMM [21,26,31,33,37,39]. First, it is essential to emphasize that the negative surface charge density has been found to increase [26] with reduced contact angle of derivatized and non-derivatized glass surfaces similar to those used here. Further, to a first approximation, on such surfaces, the effect of altered contact angle on motility may be attributed to different fractions of two different HMM configurations (Fig. 3) with minimal variation in the total HMM density [21,26,37,39]. Configuration A (Fig. 3A) is the main actin propelling configuration (see also [40]) with HMM adsorbed to the surfaces only via the conformationally instable C-terminal region. This configuration dominates on hydrophobic surfaces [21,37] (TMCS) whereas there is strong evidence [21,37] that HMM adsorbs, to a great extent, to pure glass/SiO_2 by a mechanism where positively charged loops in the actin binding region are important [26,39] (Fig. 3B; configuration B). Configuration A (Fig. 3A) becomes increasingly populated with increased contact angle and reduced negative surface charge density [21,26,37] at the expense of configuration B. In addition to configurations A and B, it is likely that there is a fraction of HMM molecules that are adsorbed to the surface both via the head and tail region [21,37,38,40,41], at least temporarily (configuration C; Fig. 3A). Whereas this fraction is likely to be low at the present, high, HMM incubation concentrations [21,39,42], configuration C may play an important role in effects of RLC phosphorylation and Ca^{2+}-binding. Thus, in terms of the model in Fig. 3, it may suffice with a small increase in the fraction of HMM molecules in configuration A to restore motility on surfaces of a contact angle of 10°. These HMM molecules would increase the fraction of myosin

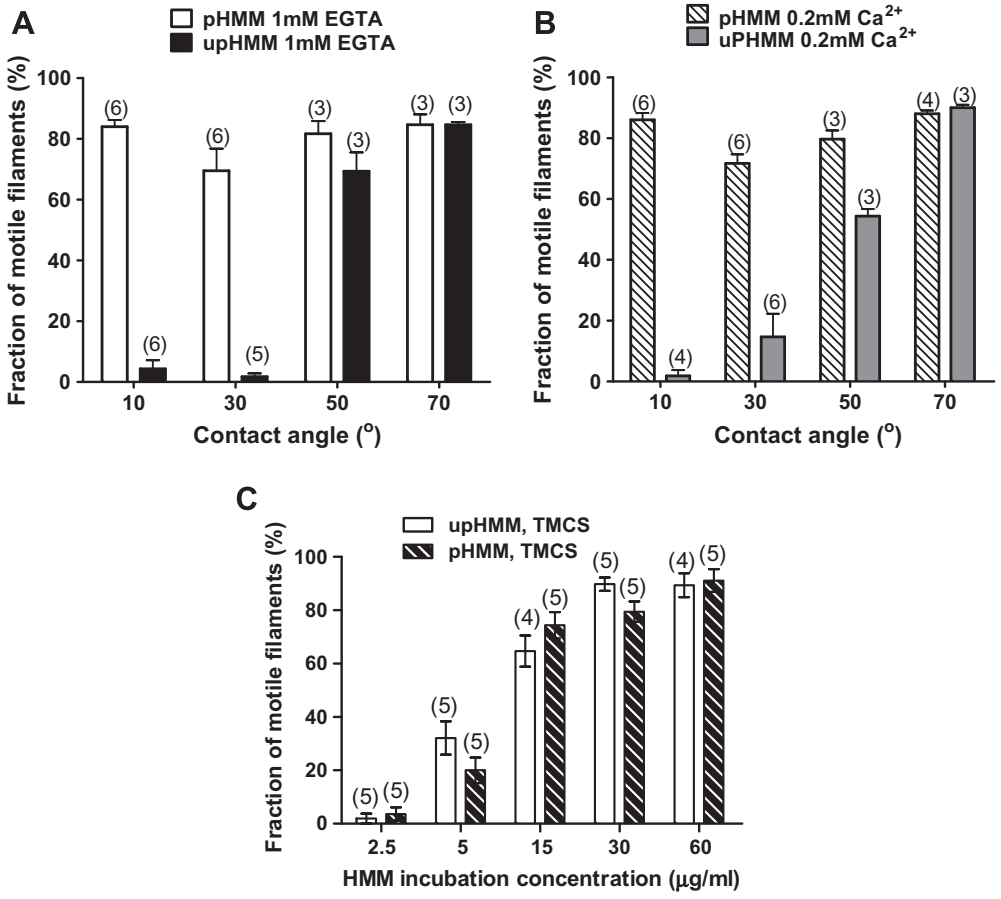

Fig. 2. Fraction of actin filaments propelled by pHMM and upHMM. (A) In the absence of Ca^{2+} at different surface contact angles, (B) as in A but in the presence of 0.2 mM Ca^{2+}. Numbers in parentheses refer to the number of flow cell regions examined. (C) Fraction of actin filaments propelled by pHMM and upHMM after incubation of TMCS surface with different HMM concentrations. Five flow cell regions examined at each concentration; one experimental date.

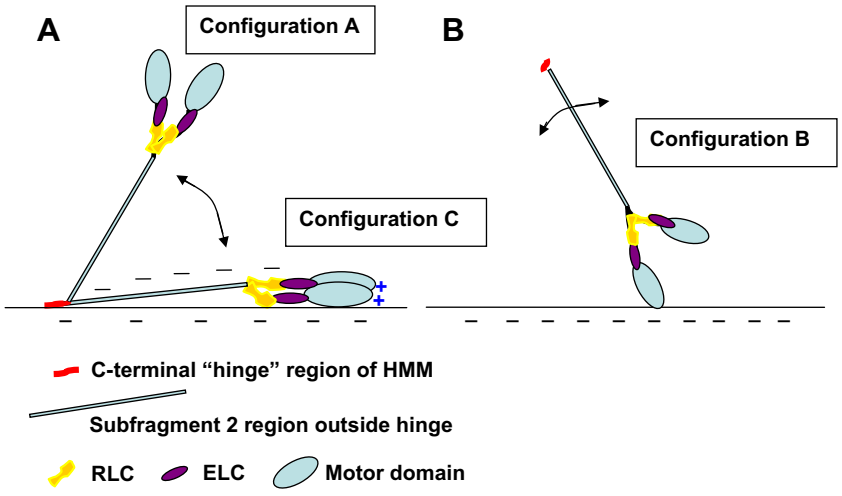

Fig. 3. Model for HMM adsorption to artificial surfaces. (A) HMM configuration A where HMM adsorbs to the surface via the C-terminal tail region (the "hinge") and executes thermal motion (curved arrow) around this attachment point with the potential to hit the surface with the head part and temporarily adsorb via a second point in the head/neck region (configuration C). Charge distribution along different parts of the HMM molecule schematically indicated as well as the negative surface charge density. (B) HMM configuration B where HMM adsorbs to the surface via positively charged actin binding region and executes thermal motion (curved arrow) around this point or around the neck–tail junction.

heads that, at least temporarily (*cf.* [21]), reach above the tails of the HMM molecules in configuration B to bind actin. That only a *small* increase of the configuration A fraction is required is suggested by the existence of some motile filaments with upHMM at the second lowest contact angle studied (30°). Further evidence that only a small fraction of the HMM molecules need to be in configuration A for reasonable motility quality is provided by the data in Fig. 4 where it can be seen that the sliding velocity of actin filaments propelled by pHMM on a surface of contact angle 30° (0 mM Ca^{2+}; see [31] for similar results with upHMM) was lower for short

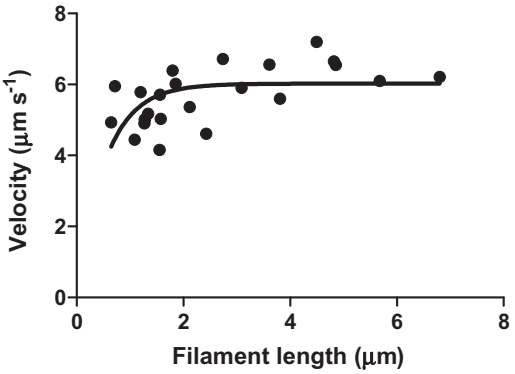

Fig. 4. HMM induced actin filament sliding velocity *vs.* filament length. Actin filaments propelled by pHMM adsorbed to a surface of 30° contact angle. Line represents fit of Eq. (1) to experimental data.

than long filaments. This suggests (from fitting of Eq. (1)) that the surface density of pHMM molecules with *actin propelling capability* was quite low (460 μm^{-2}) compared to that on TMCS (>5000 μm^{-2}; see Supplementary material).

The fraction of HMM molecules in configuration A could increase if phosphorylation of the RLCs cause changes in the myosin head, e.g. altered electrostatic surface potential or structural changes [13,43], that would reduce the affinity of the head to pure glass surfaces (*cf.* [21,39]). The effect would be an equilibrium shift from configuration C to configuration A and/or reduced initial adsorption into configuration B. This is in accordance with the findings in Fig. 2 that pHMM rescues actin filament motility on surfaces of low contact angle but not on TMCS derivatized surfaces with low HMM surface density (Fig. 2C). Thus, in the latter case the low velocity is due to the overall low HMM density, whereas a dominant fraction of the HMM molecules are likely to be in configuration A, independent of phosphorylation status.

Further mechanistic insight and critical tests of the proposed model may be possible in future studies by reversible phosphorylation/dephosphorylation using myosin light chain kinase/phosphatase systems. Such experiments could also be an important step towards phosphorylation based control of motility in nanotechnological applications. For instance, using TMCS-tracks as described previously [22], patches of pure SiO_2 (hydrophilic, negatively charged) may be inserted by appropriate nanofabrication along short stretches of the tracks. Overall change in phosphorylation of HMM on the entire surface (by adding constitutively active MLCK or phosphatase) would now be expected to substantially affect motility only on the SiO_2 parts of the tracks, allowing local and temporary stopping (to pick up cargoes) and starting of actin filament sliding (see also [24,25]). An interesting alternative to MLCK/phosphatase based control, e.g. if enzyme diffusion is hindered by a dense HMM layer [21], would be to engineer light sensitive groups into the RLCs to mimic the phosphorylation induced structural changes upon proper illumination (*cf.* [44]).

In conclusion, our results support the ideas that phosphorylation induced modulation of myosin propelled actin filament sliding via the regulatory light chains, but not effects attributed to Ca^{2+}–Mg^{2+} exchange, is potentially useful in nanotechnological applications. Additionally, the results suggest that Ca^{2+}–Mg^{2+} exchange and phosphorylation of the RLCs affect the actomyosin interaction by different and independent molecular mechanisms.

Acknowledgments

The work was supported by The Swedish Research Council (Project # 621-2007-6137), The Carl Trygger Foundation, The Knowledge Foundation (KK-stiftelsen), The Crafoord Foundation, Magnus Bergvall Foundation, Sparbanksstiftelsen Kronan and The Faculty of Natural Sciences and Engineering, University of Kalmar and Linnaeus University. Discussions with Professor Sven Tågerud are gratefully acknowledged.

Appendix A. Supplementary material

Supplementary data associated with this article can be found, in the online version, at doi:10.1016/j.bbrc.2010.10.039.

References

[1] I. Rayment, W.R. Rypniewski, K. Schmidt-Base, R. Smith, D.R. Tomchick, M.M. Benning, D.A. Winkelmann, G. Wesenberg, H.M. Holden, Three-dimensional structure of myosin subfragment-1: a molecular motor, Science 261 (1993) 50–58.
[2] X. Xie, D.H. Harrison, I. Schlichting, R.M. Sweet, V.N. Kalabokis, A.G. Szent-Gyorgyi, C. Cohen, Structure of the regulatory domain of scallop myosin at 2.8 Å resolution, Nature 368 (1994) 306–312.
[3] M.A. Geeves, K.C. Holmes, The molecular mechanism of muscle contraction, Adv. Protein Chem. 71 (2005) 161–193.
[4] J.R. Sellers, Regulation of cytoplasmic and smooth muscle myosin, Curr. Opin. Cell Biol. 3 (1991) 98–104.
[5] D.M. Himmel, S. Mui, E. O'Neall-Hennessey, A.G. Szent-Gyorgyi, C. Cohen, The on-off switch in regulated myosins: different triggers but related mechanisms, J. Mol. Biol. 394 (2009) 496–505.
[6] A.M. Gordon, E. Homsher, M. Regnier, Regulation of contraction in striated muscle, Physiol. Rev. 80 (2000) 853–924.
[7] H.L. Sweeney, B.F. Bowman, J.T. Stull, Myosin light chain phosphorylation in vertebrate striated muscle: regulation and function, Am. J. Physiol. 264 (1993) C1085–C1095.
[8] C.R. Bagshaw, On the location of the divalent metal binding sites and the light chain subunits of vertebrate myosin, Biochemistry 16 (1977) 59–67.
[9] D. Stepkowski, The role of the skeletal muscle myosin light chains N-terminal fragments, FEBS Lett. 374 (1995) 6–11.
[10] D. Szczesna, D. Ghosh, Q. Li, A.V. Gomes, G. Guzman, C. Arana, G. Zhi, J.T. Stull, J.D. Potter, Familial hypertrophic cardiomyopathy mutations in the regulatory light chains of myosin affect their structure, Ca2+ binding and phosphorylation, J. Biol. Chem. 276 (2001) 7086–7092.
[11] D. Szczesna, J. Zhao, M. Jones, G. Zhi, J. Stull, J.D. Potter, Phosphorylation of the regulatory light chains of myosin affects Ca2+ sensitivity of skeletal muscle contraction, J. Appl. Physiol. 92 (2002) 1661–1670.
[12] Z. Podlubnaya, I. Kakol, A. Moczarska, D. Stepkowski, S. Udaltsov, Calcium-induced structural changes in synthetic myosin filaments of vertebrate striated muscles, J. Struct. Biol. 127 (1999) 1–15.
[13] H.L. Sweeney, Z. Yang, G. Zhi, J.T. Stull, K.M. Trybus, Charge replacement near the phosphorylatable serine of the myosin regulatory light chain mimics aspects of phosphorylation, Proc. Natl. Acad. Sci. USA 91 (1994) 1490–1494.
[14] M.J. Greenberg, T.R. Mealy, J.D. Watt, M. Jones, D. Szczesna-Cordary, J.R. Moore, The molecular effects of skeletal muscle myosin regulatory light chain phosphorylation, Am. J. Physiol. Regul. Integr. Comp. Physiol. 297 (2009) R265–R274.
[15] M. Stewart, K. Franks-Skiba, R. Cooke, Myosin regulatory light chain phosphorylation inhibits shortening velocities of skeletal muscle fibers in the presence of the myosin inhibitor blebbistatin, J. Muscle Res. Cell Motil. 30 (2009) 17–27.
[16] Z.A. Podlubnaya, S.L. Malyshev, K. Nieznanski, D. Stepkowski, Order-disorder structural transitions in synthetic filaments of fast and slow skeletal muscle myosins under relaxing and activating conditions, Acta Biochim. Pol. 47 (2000) 1007–1017.
[17] R.J. Levine, Z. Yang, N.D. Epstein, L. Fananapazir, J.T. Stull, H.L. Sweeney, Structural and functional responses of mammalian thick filaments to alterations in myosin regulatory light chains, J. Struct. Biol. 122 (1998) 149–161.
[18] Z. Yang, J.T. Stull, R.J. Levine, H.L. Sweeney, Changes in interfilament spacing mimic the effects of myosin regulatory light chain phosphorylation in rabbit psoas fibers, J. Struct. Biol. 122 (1998) 139–148.
[19] J.M. Metzger, R.L. Moss, Myosin light chain 2 modulates calcium-sensitive cross-bridge transitions in vertebrate skeletal muscle, Biophys. J. 63 (1992) 460–468.
[20] M. Wrotek, S. Borovikov Yu, N.N. Lebedeva, I. Kakol, Some properties of glycerinated skeletal muscle fibers containing phosphorylated myosin, Gen. Physiol. Biophys. 8 (1989) 569–578.
[21] M. Persson, N. Albet-Torres, M. Sundberg, L. Ionov, S. Diez, F. Höök, A. Månsson, M. Balaz, Heavy Meromyosin Molecules Extend more than 50 nm above Adsorbing Electronegative Surfaces, Langmuir 26 (2010) 9927–9936.
[22] M. Sundberg, R. Bunk, N. Albet-Torres, A. Kvennefors, F. Persson, L. Montelius, I.A. Nicholls, S. Ghatnekar-Nilsson, P. Omling, S. Tagerud, A. Mansson, Actin filament guidance on a chip: toward high-throughput assays and lab-on-a-chip applications, Langmuir 22 (2006) 7286–7295.
[23] A. Månsson, M. Sundberg, R. Bunk, M. Balaz, I.A. Nicholls, P. Omling, J.O. Tegenfeldt, S. Tågerud, L. Montelius, Actin-based molecular motors for cargo

transportation in nanotechnology – potentials and challenges, IEEE Trans. Adv. Pack. 28 (2005) 547–555.
[24] A. Agarwal, H. Hess, Biomolecular motors at the intersection of nanotechnology and polymer science, Prog. Polym. Sci. 35 (2010) 252–277.
[25] C. Brunner, C. Wahnes, V. Vogel, Cargo pick-up from engineered loading stations by kinesin driven molecular shuttles, Lab Chip 7 (2007) 1263–1271.
[26] N. Albet-Torres, J. O'Mahony, C. Charlton, M. Balaz, P. Lisboa, T. Aastrup, A. Mansson, I.A. Nicholls, Mode of heavy meromyosin adsorption and motor function correlated with surface hydrophobicity and charge, Langmuir 23 (2007) 11147–11156.
[27] D. Stepkowski, D. Szczesna, M. Wrotek, I. Kakol, Factors influencing interaction of phosphorylated and dephosphorylated myosin with actin, Biochim. Biophys. Acta 831 (1985) 321–329.
[28] S.J. Kron, Y.Y. Toyoshima, T.Q. Uyeda, J.A. Spudich, Assays for actin sliding movement over myosin-coated surfaces, Methods Enzymol. 196 (1991) 399–416.
[29] J.D. Pardee, J.A. Spudich, Purification of muscle actin., Methods Enzymol. 85 (1982) 164–181. Pt B.
[30] W.T. Perrie, S.V. Perry, An electrophoretic study of the low-molecular-weight components of myosin, Biochem. J. 119 (1970) 31–38.
[31] M. Sundberg, M. Balaz, R. Bunk, J.P. Rosengren-Holmberg, L. Montelius, I.A. Nicholls, P. Omling, S. Tagerud, A. Mansson, Selective spatial localization of actomyosin motor function by chemical surface patterning, Langmuir 22 (2006) 7302–7312.
[32] D.Y. Kwok, A.W. Neumann, Contact angle measurement and contact angle interpretation, Adv. Colloid Interface Sci. 81 (1999) 167–249.
[33] M. Balaz, M. Sundberg, M. Persson, J. Kvassman, A. Månsson, Effects of surface adsorption on catalytic activity of heavy meromyosin studied using fluorescent ATP analogue, Biochemistry 46 (2007) 7233–7251.
[34] M. Sundberg, J.P. Rosengren, R. Bunk, J. Lindahl, I.A. Nicholls, S. Tagerud, P. Omling, L. Montelius, A. Mansson, Silanized surfaces for in vitro studies of actomyosin function and nanotechnology applications, Anal. Biochem. 323 (2003) 127–138.
[35] T.Q. Uyeda, S.J. Kron, J.A. Spudich, Myosin step size, estimation from slow sliding movement of actin over low densities of heavy meromyosin, J. Mol. Biol. 214 (1990) 699–710.
[36] A. Mansson, S. Tagerud, Multivariate statistics in analysis of data from the in vitro motility assay, Anal. Biochem. 314 (2003) 281–293.
[37] N. Albet-Torres, A. Gunnarsson, M. Persson, M. Balaz, F. Höök, A. Månsson, Molecular motors on lipid bilayers and silicon dioxide: different driving forces for adsorption, Soft Matter 6 (2010) 3211–3219.
[38] D.V. Nicolau, G. Solana, M. Kekic, F. Fulga, C. Mahanivong, J. Wright, C. Dos Remedios, Surface hydrophobicity modulates the operation of actomyosin-based dynamic nanodevices, Langmuir 23 (2007) 10846–10854.
[39] A. Mansson, M. Balaz, N. Albet-Torres, K.J. Rosengren, In vitro assays of molecular motors–impact of motor-surface interactions, Front. Biosci. 13 (2008) 5732–5754.
[40] Y.Y. Toyoshima, How are myosin fragments bound to nitrocellulose film?, Adv Exp. Med. Biol. 332 (1993) 259–265.
[41] G. Offer, P. Knight, The structure of the head–tail junction of the myosin molecule, J. Mol. Biol. 256 (1996) 407–416.
[42] K. Nakanishi, T. Sakiyama, K. Imamura, On the adsorption of proteins on solid surfaces, a common but very complicated phenomenon, J. Biosci. Bioeng. 91 (2001) 233–244.
[43] S. Highsmith, Myosin regulatory light chain and nucleotide modulation of actin binding site electric charge, Biochemistry 36 (1997) 2010–2016.
[44] A. Kocer, M. Walko, W. Meijberg, B.L. Feringa, A light-actuated nanovalve derived from a channel protein, Science 309 (2005) 755–758.